Graphing better Impulse Response Functions for discrete-time linear models

Gray Calhoun*
Iowa State University

2015-02-22b

Abstract

We show how to construct continuous and differentiable Impulse Response Functions and for discrete-time VARs and Vector Error-Correction Models. Current methods produce piecewise linear functions that introduce visual distortions, especially when many response functions are plotted in the same graph to represent uncertainty or partial identification. We also show how to plot the cumulative response to a shock. In addition to being more accurate than current methods, our proposed approach is also much more attractive.

1 Introduction

Impulse Response Functions (IRFs) are widely used in Macroeconomics to represent the dynamic effect over time of an unanticipated shock to an economic system. Formally, if $\{y_t\}$ is a stationary sequence of random vectors in $\mathbb{R}^k$ and

$$\mathrm{E}(y_{t+s} \mid y_t, y_{t-1}, \dots) = g_s(y_t, \dots, y_{t-p})$$

for each $s > 0$,[1] the IRF corresponding to the shock Δ is the difference

$$\Psi_s(\Delta) = g_s(y_t + \Delta, y_{t-1}, \dots, y_{t-p}) - g_s(y_t, y_{t-1}, \dots, y_{t-p})$$

viewed as a function of s.[2] Obviously the values of the IRF depend on the specific nature of the shock Δ, and different choices of Δ can correspond to different shocks of

*Economics Department; Iowa State University; Ames, IA 50011. Telephone: (515) 294-6271. Email: «gcalhoun@iastate.edu», web: «http://www.econ.iastate.edu/~gcalhoun».

[1] For later convenience, define $g_0(y_t, \dots, y_{t-p}) = y_t$ and $g_s = 0$ for $s < 0$.

[2] Note that $\Psi_0(\Delta) = \Delta$ and $\Psi_s(\Delta) = 0$ for $s < 0$.

theoretical interest. In Macroeconomic applications, t and s are typically integers and g_s is often derived from a recursive linear model, the VAR

$$y_t = A_0 + A_1 y_{t-1} + \cdots + A_p y_{t-p} + \varepsilon_t \tag{1}$$

where ε_t is a martingale difference sequence is one example.

It is straightforward to calculate the values of the IRFs for integer-values of s in models like (1). Note that

$$\begin{aligned} g_1(y_t, \ldots, y_{t-p}) &= \mathrm{E}(y_{t+1} \mid y_t, y_{t-1}, \ldots) \\ &= A_0 + A_1 y_t + \cdots + A_p y_{t-p+1} \end{aligned}$$

and

$$\begin{aligned} g_s(y_t, \ldots, y_{t-p}) &= \mathrm{E}(y_{t+s} \mid y_t, y_{t-1}, \ldots) \\ &= \mathrm{E}(\mathrm{E}(y_{t+s} \mid y_{t+s-1}, y_{t+s-2}, \ldots) \mid y_t, y_{t-1}, \ldots) \\ &= \mathrm{E}(A_0 + A_1 y_{t+s-1} + \cdots + A_p y_{t+s-p} \mid y_t, y_{t-1}, \ldots) \\ &= A_0 + A_1 \mathrm{E}(y_{t+s-1} \mid y_t, y_{t-1}, \ldots) + \cdots + A_p \mathrm{E}(y_{t+s-p} \mid y_t, y_{t-1}, \ldots) \\ &= A_0 + A_1 g_{s-1}(y_t, \ldots, y_{t-p}) + \cdots + A_p g_{s-p}(y_t, \ldots, y_{t-p}) \end{aligned}$$

for $s > 1$, which can be calculated recursively for $s = 2, 3, \ldots$. Then

$$\Psi_1(\Delta) = A_1 \Delta$$

and, for $s > 1$,

$$\begin{aligned} \Psi_s(\Delta) &= g_s(y_t + \Delta, \ldots, y_{t-p}) - g_s(y_t, \ldots, y_{t-p}) \\ &= \sum_{\ell=1}^{p} A_\ell [g_{s-\ell}(y_t + \Delta, \ldots, y_{t-p}) - g_{s-\ell}(y_t, \ldots, y_{t-p})] \\ &= \sum_{\ell=1}^{p} A_\ell \Psi_{s-\ell}(\Delta) \end{aligned}$$

which can again be calculated recursively. In some applications this is enough. But in most applications, it is necessary to graph the IRFs and to connect the points; this is especially important when more than one IRF is plotted on the same graph — whether to represent dynamics under different assumptions (see Bernanke and Mihov, 1998, and Stock and Watson, 2001, for representative examples), to represent statistical uncertainty (Kilian, 1998, and Sims and Zha, 1999) or to represent regions that are partially identified (Uhlig, 2005, and Inoue and Kilian, 2013). So far, representing these dynamics has been achieved by linear interpolation, so

$$\Psi_s(\Delta) = (s - \mathrm{floor}(s))\, \Psi_{\mathrm{ceil}(s)}(\Delta) + (\mathrm{ceil}(s) - s)\, \Psi_{\mathrm{floor}(s)}(\Delta)$$

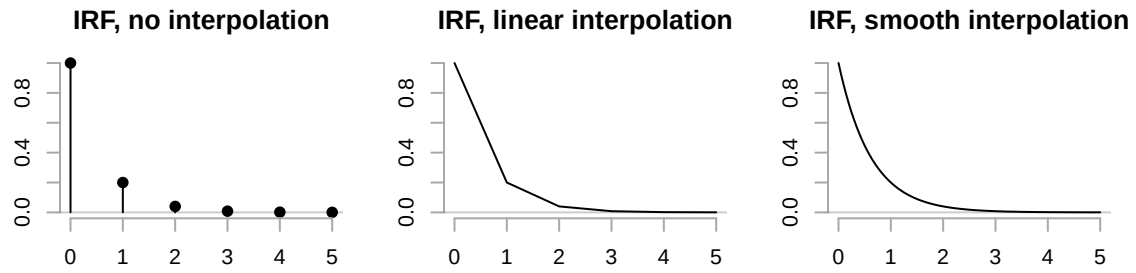

Figure 1: IRF for simple AR(1) example. Here $y_t = 0.2y_{t-1} + \varepsilon_t$ — the vertical axis shows $\Psi_x(1)$. The left panel plots only integer values of x, the middle panel uses linear interpolation between the integers, and the right panel plots the function 0.2^x directly.

for noninteger s, where floor(s) and ceil(s) represent the largest integer less than s and smallest integer value greater than s respectively. Unfortunately, this method introduces misleading visual distortions, which we will explicitly discuss later.

In this paper, we show how the IRF $\Psi_s(\Delta)$ can be meaningfully defined for VARs for any real positive value of s and give a convenient method for calculating it. (Figures 3 and 4 have examples if you're impatient to see them.) This allows researchers to use the VAR itself to interpolate between the points for which it is usually defined and results in graphs that do not have the distortions produced by linear interpolation. In the next section, we offer a simple example of our approach that motivates the general technique. Sections 3 and 4 explain the methods in general and provide some extensions to cumulative responses and Vector Error Correction Models, and Section 5 provides a numerical example.

2 Motivation

For motivation, start with the simplest univariate case and assume that y_t is the AR(1)

$$y_t = a y_{t-1} + \varepsilon_t$$

It is well-known that the recursive definitions used in the first section imply that $\Psi_s(\Delta) = a^s\Delta$. When $a > 0$, this function is well-defined for all positive real s, and can be used directly to interpolate between the integer points. Figure 1 plots $\Psi_s(\Delta)$ for $\Delta = 1$ and $a = 0.2$ using three approaches: first only for the integer values of s, second using linear interpolation between the integer values, and finally using $a^s\Delta$ directly for all $s \geq 0$.[3] While one could debate which of the functions represents the "true" impact at a fractional point in time, the right panel — using 0.2^s directly — more clearly expresses the shock's rate of decay and, equivalently, the dynamics of the AR model.

[3]All of the graphs in this paper were produced using R Development Core Team (2011)

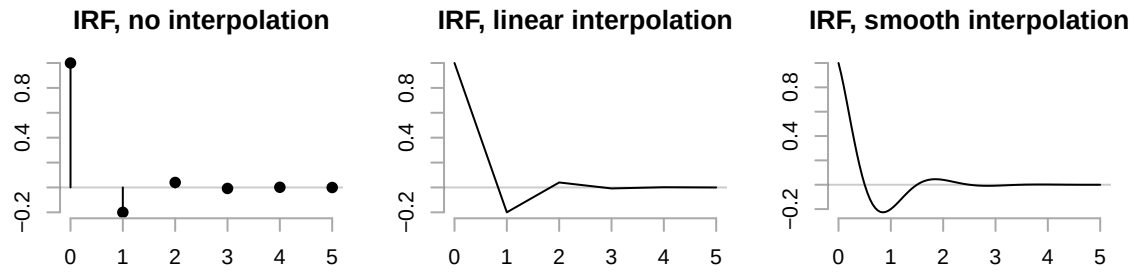

Figure 2: IRF for simple AR(1) example. Here $y_t = -0.2y_{t-1} + \varepsilon_t$ — the vertical axis shows $\Psi_x(1)$. The left panel plots only integer values of x, the middle panel uses linear interpolation between the integers, and the right panel plots the function $|a|^x \cos(\pi x)$ directly.

This clarity should not be surprising. We can see that $\Psi_s(\Delta) = a^s\Delta$ satisfies the recurrence relation implied by the lag structure of the original AR process for any positive real value of s:

$$\Psi_s(\Delta) = a^s\Delta = a \times a^{s-1}\Delta = a\,\Psi_{s-1}(\Delta).$$

For the methods we propose in this paper we will see that this condition holds in general: if $\Phi(L)$ is the lag polynomial of the VAR(so $\Phi(L)y_t = \varepsilon_t$ for $t = 1, 2, \dots$), then $\Phi(L)\Psi_s(\Delta) = 0$ for all $s \in \mathbb{R}^+$.[4] This condition only holds for integer values of s when $\Psi_s(\Delta)$ is constructed by linear interpolation.

The case $a \in (-1, 0)$ is slightly more complicated. The previous solution, $a^s\Delta$, continues to be well-defined and has a real value for all integer values of s, but is not for non-integer values. However, for any integer value of s the equality

$$a^s = |a|^s \cos(\pi s)$$

holds, so $\Psi_s(\Delta) = |a|^s \cos(\pi s)\Delta$ agrees with $a^s\Delta$ on integer values and is well-defined and real-valued for non-integer values. Moreover, this choice of $\Psi_s(\Delta)$ satisfies the recurrence relation for the AR(1) model (when $a < 0$) just as before:

$$\Psi_s(\Delta) = |a|^s \cos(\pi s) \cdot \Delta = -|a| \times |a|^{s-1} \cos(\pi(s-1)) \cdot \Delta = a\,\Psi_{s-1}(\Delta)$$

implying

$$(1 - aL)\,\Psi_s(\Delta) = 0.$$

Since it is exactly correct on the integers and satisfies the model's dynamics for noninteger values as well, this choice of Ψ is a sensible choice for interpolating between the integers. Figure 2 plots the IRFs for $a = -0.2$ and $\Delta = 1$ with no interpolation, linear interpolation, and our definition of $\Psi_s(\Delta)$. The smooth version more accurately reflects the system's dynamics again.

[4] We have implicitly defined $L\Psi_s(\Delta) = \Psi_{s-1}(\Delta)$.

This choice of $\Psi_s(\Delta)$ was not made at random. Any complex number $a + bi$ can be written in polar form,

$$a + bi = R[\cos(\theta) - i\sin(\theta)]$$

where $R = |a^2 + b^2|^{1/2}$ and θ satisfies $\cos(\theta) = a/R$ and $\sin(\theta) = b/R$; then real powers can be defined easily as[5]

$$(a + bi)^s = R^s[\cos(\theta s) - i\sin(\theta s)].$$

For the AR example above, $a < 0$ and $b = 1$ implies that $\theta = \pi$, giving $a^s = |a|^s\cos(\pi s)$ as we originally claimed. This example also suggests a more general method: for any VAR we can solve the recurrence relation using standard tools (as described in Hamilton, 1994, for example) and use that solution as the IRF for real-valued s. We pursue that approach in the next section.

3 General Approach

The AR(1) model in the previous section can be extended to general VARs using the "canonical" representation.[6] Define y_t as in Equation (1), so

$$y_t = \sum_{j=1}^{p} A_j y_{t-j} + \varepsilon_t.$$

To represent this relationship as a VAR(1), form the vector $(y_t', \ldots, y_{t-p+1}')'$ and observe that

$$\underbrace{\begin{pmatrix} y_t \\ y_{t-1} \\ y_{t-2} \\ \vdots \\ y_{t-p+1} \end{pmatrix}}_{Z_t} = \underbrace{\begin{pmatrix} A_1 & A_2 & \cdots & A_{p-1} & A_p \\ I_k & 0 & \cdots & 0 & 0 \\ 0 & I_k & \cdots & 0 & 0 \\ \vdots & \vdots & \ddots & \vdots & \vdots \\ 0 & 0 & \cdots & I_k & 0 \end{pmatrix}}_{F} \underbrace{\begin{pmatrix} y_{t-1} \\ y_{t-2} \\ y_{t-3} \\ \vdots \\ y_{t-p} \end{pmatrix}}_{Z_{t-1}} + \underbrace{\begin{pmatrix} \varepsilon_t \\ 0 \\ 0 \\ \vdots \\ 0 \end{pmatrix}}_{U_t}.$$

n So this relationship is equivalent to $Z_t = FZ_{t-1} + U_t$.

If the matrix F has q distinct eigenvalues, it can be decomposed as

$$F = MJM^{-1}$$

where J is block diagonal of the form

$$J = \begin{pmatrix} J_1 & \cdots & 0 \\ \vdots & \ddots & \vdots \\ 0 & \cdots & J_q \end{pmatrix}$$

[5] See Hamilton (1994) for an introduction.

[6] See Chapter 1 of Hamilton (1994) for a textbook treatment of much of this material.

and each J_ℓ is $m_\ell \times m_\ell$ of the form

$$J_\ell = \begin{pmatrix} \lambda_\ell & 1 & 0 & \cdots & 0 & 0 \\ 0 & \lambda_\ell & 1 & \cdots & 0 & 0 \\ 0 & 0 & \lambda_\ell & \cdots & 0 & 0 \\ \vdots & \vdots & \vdots & \ddots & \vdots & \vdots \\ 0 & 0 & 0 & \cdots & \lambda_\ell & 1 \\ 0 & 0 & 0 & \cdots & 0 & \lambda_\ell \end{pmatrix}$$

where $\lambda_1, \ldots, \lambda_q$ are the distinct eigenvalues of F and m_ℓ is the number of times the ℓth eigenvalue is repeated. If all of the eigenvalues of F are distinct, this is just the eigenvalue decomposition of F.

This representation is convenient because, for positive integer values of s, we have

$$F^s = MJ^sM^{-1}$$

and

$$J^s = \begin{pmatrix} J_1^s & \cdots & 0 \\ \vdots & \ddots & \vdots \\ 0 & \cdots & J_q^s \end{pmatrix},$$

where

$$\begin{aligned} J_\ell^s &= \begin{pmatrix} \lambda_\ell^s & \binom{s}{1}\lambda_\ell^{s-1} & \binom{s}{2}\lambda_\ell^{s-2} & \cdots & \binom{s}{m_\ell}\lambda_\ell^{s-m_\ell} \\ 0 & \lambda_\ell^s & \binom{s}{1}\lambda_\ell^{s-1} & \cdots & \binom{s}{m_\ell-1}\lambda_\ell^{s-m_\ell+1} \\ 0 & 0 & \lambda_\ell^s & \cdots & \binom{s}{m_\ell-2}\lambda_\ell^{s-m_\ell+2} \\ \vdots & \vdots & \vdots & \cdots & \vdots \\ 0 & 0 & 0 & \cdots & \lambda_\ell^s \end{pmatrix} \\ &= \begin{pmatrix} h_\ell(s,0) & h_\ell(s,1) & h_\ell(s,2) & \cdots & h_\ell(s,m_\ell) \\ 0 & h_\ell(s,0) & h_\ell(s,1) & \cdots & h_\ell(s,m_\ell-1) \\ 0 & 0 & h_\ell(s,0) & \cdots & h_\ell(s,m_\ell-2) \\ \vdots & \vdots & \vdots & \ddots & \vdots \\ 0 & 0 & 0 & \cdots & h_\ell(s,0) \end{pmatrix} \end{aligned}$$

and

$$h_\ell(s,j) = \begin{cases} |\lambda_\ell|^s[\cos(\theta_\ell s) + i\sin(\theta_\ell s)] & j = 0 \\ \frac{s!}{j!(s-j)!}|\lambda_\ell|^s[\cos(\theta_\ell s) + i\sin(\theta_\ell s)] & \text{if } s \geq j > 0 \\ 0 & \text{otherwise.} \end{cases}$$

where $\cos(\theta_\ell) = \mathrm{Re}(\lambda_\ell)/|\lambda_\ell|$ and $\sin(\theta_\ell) = \mathrm{Im}(\lambda_\ell)/|\lambda_\ell|$ as above.

Then we can write

$$F^s = \sum_{j=1}^{q} \sum_{l=0}^{\min(m_\ell, \text{floor}(s))} \frac{s(s-1)\cdots(s-l+1)}{l(l-1)\cdots 1} |\lambda_j|^{s-l} \times \left\{ [A_{jl}\cos(\theta_j s) + B_{jl}\sin(\theta_j s)] + i[C_{jl}\cos(\theta_j s) + D_{jl}\sin(\theta_j s)] \right\} \quad (2)$$

where the coefficient matrices A_{jl}, B_{jl}, C_{jl}, and D_{jl} are chosen to match $F^0, F^1, F^2, \ldots$. For integer values of s, the imaginary components of MJ^sM^{-1} exactly cancel, so

$$0 = \sum_{j=1}^{q} \sum_{l=0}^{\min(m_\ell, \text{floor}(s))} \frac{s(s-1)\cdots(s-l+1)}{l(l-1)\cdots 1} |\lambda_j|^{s-l} [C_{jl}\cos(\theta_j s) + D_{jl}\sin(\theta_j s)]$$

and we can use the real part alone, giving

$$F^s = \sum_{j=1}^{q} \sum_{l=0}^{\min(m_\ell, \text{floor}(s))} \frac{s(s-1)\cdots(s-l+1)}{l(l-1)\cdots 1} |\lambda_j|^{s-l} [A_{jl}\cos(\theta_j s) + B_{jl}\sin(\theta_j s)] \quad (3)$$

to produce $F^1, F^2, F^3, \ldots$. Our proposal, in a nutshell, is to use the definition given by (3) for all of the reals rather than just the integers, exactly as we did in the motivating AR(1) examples.

Equation (2) has another practical implication. Although F^s has real and imaginary components for real s, we are only interested in its real component, which generates the IRFs for integer values of s. So rather than working out the matrices A_{jl} and B_{jl} to use (3), we can calculate the complex valued F^s and simply drop its imaginary component. This calculation is directly available in many programming languages and can be implemented as MJ^sM^{-1} using the Jordan decomposition if it is not.

We conclude this section with a formal statement of the result.

Proposition 1 (Impulse Response Functions for VARs)**.** *Let F be the coefficient matrix of the canonical VAR(1) representation of an arbitrary VAR(p), and let M and J be the matrices of its Jordan decomposition, so $F = MJM^{-1}$. Define $\Psi_s(\Delta)$ as the first k elements of the vector $\text{Re}(MJ^sM^{-1})\Delta_0$ for all $s \in [0, +\infty)$, where $\Delta_0 = (\Delta', 0')'$.*

Then

$$\Psi_s(\Delta) = \sum_{j=1}^{q} A_j \Psi_{s-j}(\Delta)$$

for all $s > 0$, so $\Psi_s(\Delta)$ satisfies the recurrence relation implied by the original VAR.

Proof. Observe that the series $a_s = \text{Re}(F^s)\Delta_0$ satisfies $a_s = Fa_{s-1}$, since F is real and

$$Fa_{s-1} = F\,\text{Re}(F^{s-1})\Delta_0 = \text{Re}(F^s)\Delta_0 = a_s.$$

The conclusion of this proposition is a direct consequence. □

4 Cumulative response and other extensions

The results in the previous section will work for many applications, but in others we may may be interested in other functions of the variables. An example is if y_t represents differenced variables, (say, the first difference of log GDP), but we are interested in the response on the level of the variable. A different but very similar issue arises if the model of interest is a Vector Error Correction Model (VECM) model and not a VAR. In these cases, we can augment the canonical form used earlier to derive a new VAR(1) representation, and then apply our earlier techniques. We'll demonstrate this approach for these two examples.

First, suppose that y_t has a stationary VAR(p) representation as before, but now we want to derive the response on some elements of the vector $S_t = \sum_{s=0}^{t} y_s$. Immediately we have $S_t - y_t = S_{t-1}$, so we can extend the canonical representation for y_t by adding S_t as the first element of the vector Z_t. Observe that

$$\begin{pmatrix} S_t - y_t \\ y_t \\ y_{t-1} \\ y_{t-2} \\ \vdots \\ y_{t-p+1} \end{pmatrix} = \begin{pmatrix} I & 0 & 0 & \cdots & 0 & 0 \\ 0 & A_1 & A_2 & \cdots & A_{p-1} & A_p \\ 0 & I & 0 & \cdots & 0 & 0 \\ 0 & 0 & I & \cdots & 0 & 0 \\ \vdots & \vdots & \vdots & \ddots & \vdots & \vdots \\ 0 & 0 & 0 & \cdots & I & 0 \end{pmatrix} \begin{pmatrix} S_{t-1} \\ y_{t-1} \\ y_{t-2} \\ \vdots \\ y_{t-p+1} \\ y_{t-p} \end{pmatrix} + \begin{pmatrix} 0 \\ \varepsilon_t \\ 0 \\ 0 \\ \vdots \\ 0 \end{pmatrix}.$$

And this equation can be rewritten as

$$\begin{pmatrix} S_t \\ y_t \\ y_{t-1} \\ y_{t-2} \\ \vdots \\ y_{t-p+1} \end{pmatrix} = \begin{pmatrix} I & A_1 & A_2 & \cdots & A_{p-1} & A_p \\ 0 & A_1 & A_2 & \cdots & A_{p-1} & A_p \\ 0 & I & 0 & \cdots & 0 & 0 \\ 0 & 0 & I & \cdots & 0 & 0 \\ \vdots & \vdots & \vdots & \ddots & \vdots & \vdots \\ 0 & 0 & 0 & \cdots & I & 0 \end{pmatrix} \begin{pmatrix} S_{t-1} \\ y_{t-1} \\ y_{t-2} \\ \vdots \\ y_{t-p+1} \\ y_{t-p} \end{pmatrix} + \begin{pmatrix} \varepsilon_t \\ \varepsilon_t \\ 0 \\ 0 \\ \vdots \\ 0 \end{pmatrix}.$$

This representation is now a VAR(1) that can be handled exactly as above.

The VECM model is similar. Suppose now that we have the stationary relationship

$$\Delta y_t = B y_{t-1} + A_1 \Delta y_{t-1} + \cdots + A_p \Delta y_{t-p} + \varepsilon_t.$$

This can also be put in a canonical form using almost identical arguments as before

$$\begin{pmatrix} y_t \\ \Delta y_t \\ \Delta y_{t-1} \\ \Delta y_{t-2} \\ \vdots \\ \Delta y_{t-p+1} \end{pmatrix} = \begin{pmatrix} (I+B) & A_1 & A_2 & \cdots & A_{p-1} & A_p \\ B & A_1 & A_2 & \cdots & A_{p-1} & A_p \\ 0 & I & 0 & \cdots & 0 & 0 \\ 0 & 0 & I & \cdots & 0 & 0 \\ \vdots & \vdots & \vdots & \ddots & \vdots & \vdots \\ 0 & 0 & 0 & \cdots & I & 0 \end{pmatrix} \begin{pmatrix} y_{t-1} \\ \Delta y_{t-1} \\ \Delta y_{t-2} \\ \vdots \\ \Delta y_{t-p+1} \\ \Delta y_{t-p} \end{pmatrix} + \begin{pmatrix} \varepsilon_t \\ \varepsilon_t \\ 0 \\ 0 \\ \vdots \\ 0 \end{pmatrix}$$

In both cases, we can now define the IRF using the canonical VAR(1) representation.

5 Numerical example

For a numerical example, consider the two-variable VAR(2)

$$\begin{pmatrix} y_{1t} \\ y_{2t} \end{pmatrix} = \begin{pmatrix} -0.5 & 0.01 \\ 0.3 & 0.1 \end{pmatrix} \begin{pmatrix} y_{1,t-1} \\ y_{2,t-1} \end{pmatrix} + \begin{pmatrix} -0.2 & 0.1 \\ -0.1 & 0.0 \end{pmatrix} \begin{pmatrix} y_{1,t-2} \\ y_{2,t-2} \end{pmatrix} + \begin{pmatrix} \varepsilon_{1t} \\ \varepsilon_{2t} \end{pmatrix} \tag{4}$$

and assume for the sake of argument that $(\varepsilon_{1t}, \varepsilon_{2t}) \sim N(0, I)$ represents the shocks of interest.

As described above, we will define the smooth IRFs for a shock to the first element as

$$\begin{pmatrix} \hat{y}_{1s} \\ \hat{y}_{2s} \end{pmatrix} = \begin{pmatrix} 1 & 0 & 0 & 0 \\ 0 & 1 & 0 & 0 \end{pmatrix} M J^s M^{-1} \begin{pmatrix} 1 \\ 0 \\ 0 \\ 0 \end{pmatrix}$$

with M and J the Jordan decomposition of the matrix

$$F = \begin{pmatrix} -0.5 & 0.01 & -0.2 & 0.1 \\ 0.3 & 0.1 & -0.1 & 0.0 \\ 1.0 & 0.0 & 0.0 & 0.0 \\ 0.0 & 1.0 & 0.0 & 0.0 \end{pmatrix} \tag{5}$$

The same equations hold for the IRFs for a shock to the second element of y_t, but now the last vector should be $(0, 1, 0, 0)'$.

We plot the IRFs in Figure 3. The first column plots the standard IRFs and the second plots our proposed smooth plots. Although the general impressions from both graphs are similar, there are important differences. First, peaks and troughs are often underestimated by the standard IRFs and their timing is frequently misidentified. This is especially apparent in the first peak in the second row. Second, even the sign of the IRF can be misidentified, as we see with the immediate response of y_{1t} to a shock in y_{2t}. Finally, unless turning points in the smooth functions happen to coincide with integer values, discretizing the IRFs introduces misleading asymmetries and kinks.

These distortions are even more apparent when we graph multiple perturbations of the IRFs in the same panel, which is a common way of representing uncertainty or set-identified responses. To demonstrate this phenomenon, we generated 150 replications of the IRFs by adding independent N(0, 0.15) noise terms to each element of A, and then plotting the implied IRFs as before.

These graphs are shown in Figure 4. The same issues apparent in Figure 3 are present here as well. But there are other problems as well. In the first curve, for example, the discrete IRF shows that there is substantial negative correlation between the period 2 and period 3 estimated response and the period 3 and 4 response. But the smoothed graph makes it clear that this is driven by the timing and size of the first peak. When that peak is near period 2, the curve has time to fall noticeably before period 2, but

when the peak is closer to period 3, the curve is still rising for that interval. The actual dynamics implied by the different curves are very similar. Similar but less dramatic distortions appear in the other panels as well. In the third row, for example, the discrete IRF shows that about half of the parameter values have an initial increase in response to a y_{20} shock and half have an initial decrease, but the smooth curves show that virtually all of them have an immediate decrease, but that many start to increase very soon. The exact location of the peak that falls between periods 1 and 2 determines most of the initial dynamics, but this is impossible to see in the discrete curve.

6 Discussion

Vector Autoregressive models do not just have implications for the period-to-period dynamics of a stochastic process, they also have implications about the very short-run dynamics within periods. In this paper, we propose that researchers graph those intra-period dynamics when plotting IRFs and we give a simple method to do so, based on the VAR's canonical VAR(1) representation. Even when researchers do not want to assign any economic importance to these ultra short-run dynamics, plotting them in the IRFs minimizes visual distortions that can arise from discretizing the dynamics, especially when several IRFs are plotted over each other to represent uncertainty or set identification — see Figure 4 for an example.

References

B. S. Bernanke and I. Mihov. Measuring monetary policy. *The Quarterly Journal of Economics*, 113(3):869–902, 1998.

J. D. Hamilton. *Time Series Analysis*. Princeton University Press, 1994.

A. Inoue and L. Kilian. Inference on impulse response functions in structural VAR models. *Journal of Econometrics*, 177(1):1–13, 2013.

L. Kilian. Small-sample confidence intervals for impulse response functions. *The Review of Economics and Statistics*, 80(2):218–230, 1998.

R Development Core Team. *R: A Language and Environment for Statistical Computing*. R Foundation for Statistical Computing, Vienna, Austria, 2011. URL http://www.R-project.org/.

C. A. Sims and T. Zha. Error bands for impulse responses. *Econometrica*, 67(5):1113–1155, 1999.

J. H. Stock and M. W. Watson. Vector autoregressions. *Journal of Economic Perspectives*, 15(4):101–115, Fall 2001.

H. Uhlig. What are the effects of monetary policy on output? Results from an agnostic identification procedure. *Journal of Monetary Economics*, 52(2):381–419, March 2005.

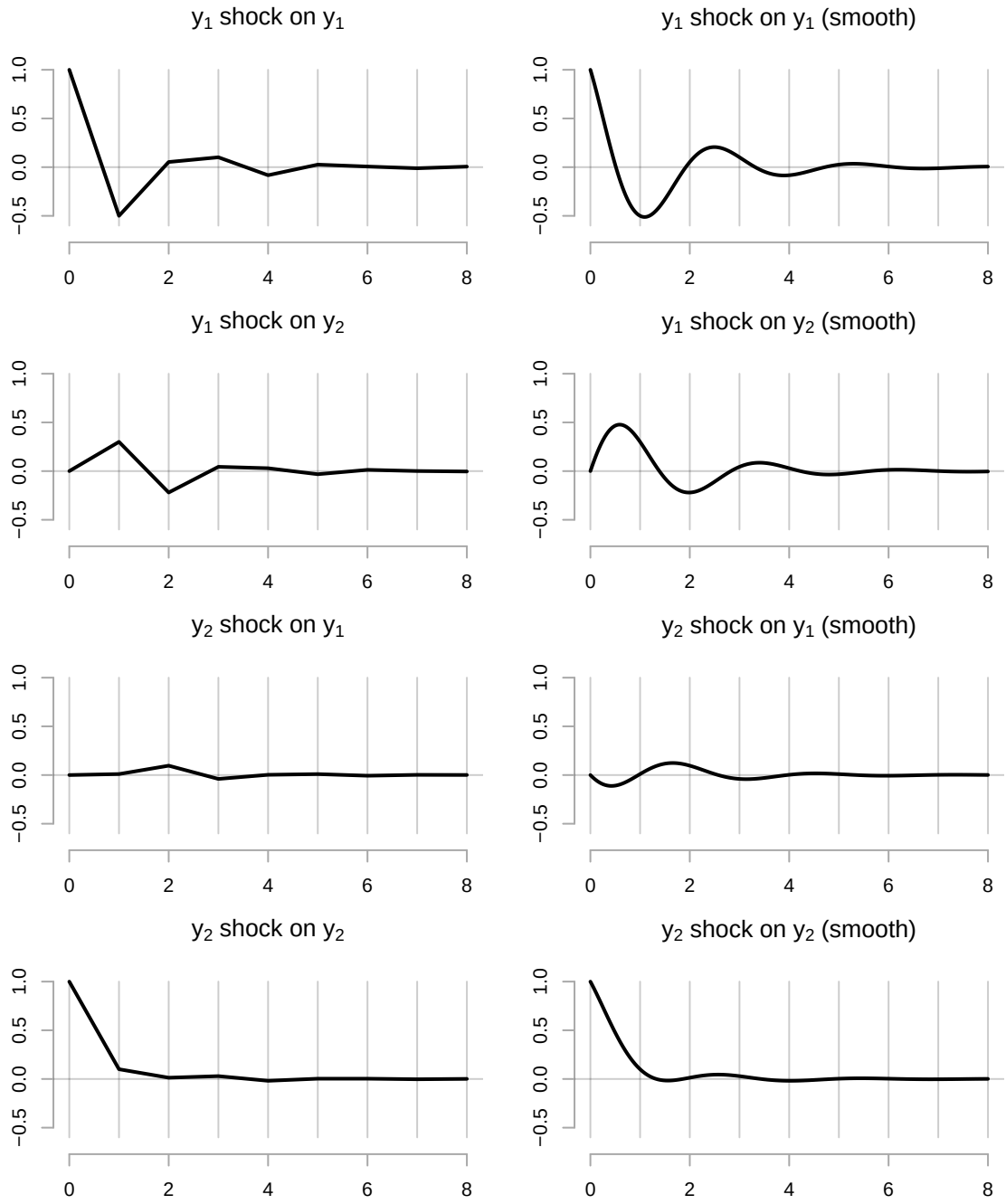

Figure 3: Impulse Response Functions from Section 5 example; y_t is generated by Equation (4). The left column plots standard IRFs and the right column plots our new method.

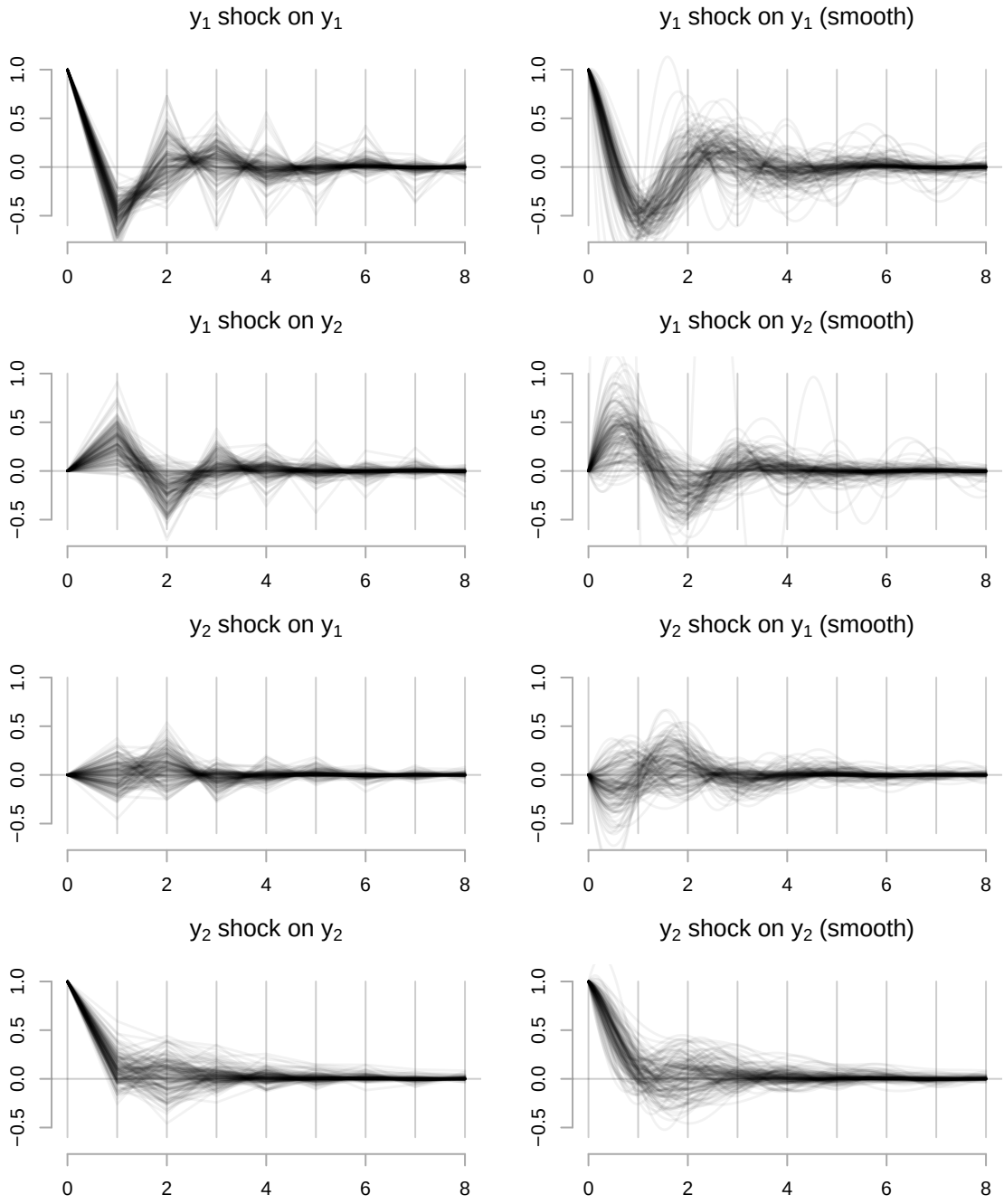

Figure 4: Impulse Response Functions from Section 5 example; y_t is generated by Equation (4), with independent $N(0, 0.15)$ random variable added to each coefficient. These graphs plot the IRFs from 150 independent draws of the coefficient matrices. The left column plots standard IRFs and the right column plots our new method.